A national laboratory of the U.S. Department of Energy
Office of Energy Efficiency & Renewable Energy

National Renewable Energy Laboratory

Innovation for Our Energy Future

Designing and Testing Controls to Mitigate Dynamic Loads in the Controls Advanced Research Turbine

Preprint

A.D. Wright
National Renewable Energy Laboratory

K.A. Stol
Department of Mechanical Engineering,
University of Auckland
Auckland, New Zealand

To be presented at the 2008 ASME Wind Energy Symposium
Reno, Nevada
January 7–10, 2008

Conference Paper
NREL/CP-500-42490
January 2008

NREL is operated by Midwest Research Institute • Battelle   Contract No. DE-AC36-99-GO10337

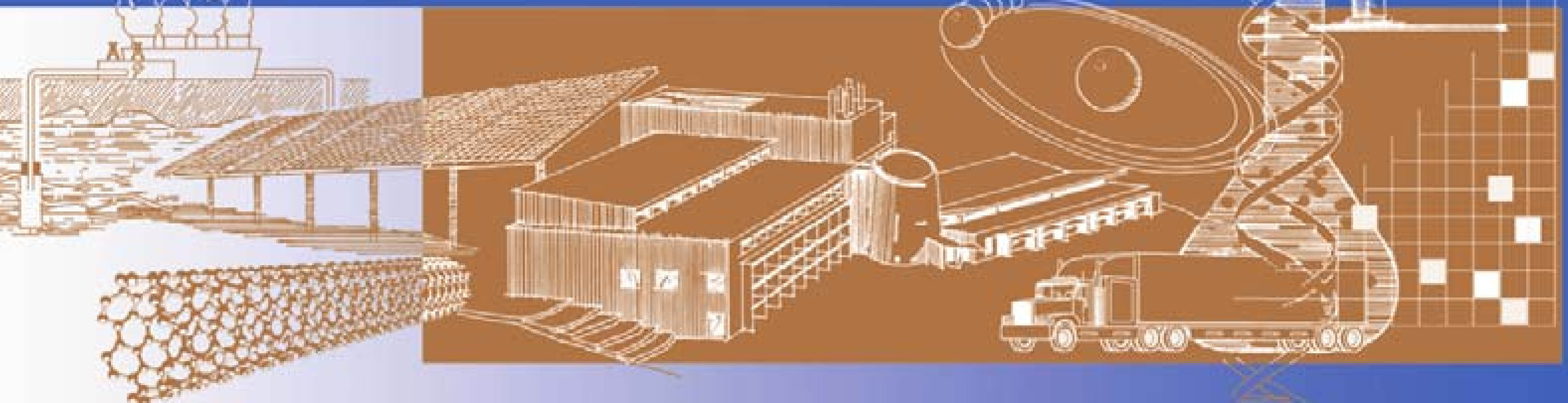

Available electronically at http://www.osti.gov/bridge

Available for a processing fee to U.S. Department of Energy
and its contractors, in paper, from:
U.S. Department of Energy
Office of Scientific and Technical Information
P.O. Box 62
Oak Ridge, TN 37831-0062
phone: 865.576.8401
fax: 865.576.5728
email: mailto:reports@adonis.osti.gov

Available for sale to the public, in paper, from:
U.S. Department of Commerce
National Technical Information Service
5285 Port Royal Road
Springfield, VA 22161
phone: 800.553.6847
fax: 703.605.6900
email: orders@ntis.fedworld.gov
online ordering: http://www.ntis.gov/ordering.htm

Printed on paper containing at least 50% wastepaper, including 20% postconsumer waste

Designing and Testing Controls to Mitigate Dynamic Loads in the Controls Advanced Research Turbine

Alan D. Wright*†
National Renewable Energy Laboratory
Golden, Colorado 80401

Karl A. Stol‡
Department of Mechanical Engineering
The University of Auckland
Private bag 92019
Auckland, New Zealand

One goal of the U.S. Department of Energy Wind Energy Program is to design fatigue-resistant wind turbines. Control systems must be developed to mitigate structural loads and reduce costs. This will enable wind energy to play a more significant part in meeting the U.S. electricity supply. Control systems that minimize fatigue loads without sacrificing turbine power while maintaining stable closed-loop behavior in the presence of turbulent wind inflow are critical for new large turbine designs.

Classical design methods such as proportional-integral-derivative control are used to design typical commercial wind turbine controllers. These methods are based on a single input and a single output. Often, multiple independent control loops are designed to meet multiple control objectives, such as speed regulation, load mitigation, and active mode damping. As wind turbines become larger and more flexible, the potential for multiple loop control systems to destabilize weakly damped flexible turbine modes increases. With modern advanced control design methods, multiple control objectives can be met with fewer control loops, leading to stable closed-loop behavior.

At the National Renewable Energy Laboratory, we are designing, implementing, and testing advanced controls to maximize energy extraction and reduce structural dynamic loads. These control designs are based on a linear model of the turbine that is generated by specialized modeling software. In this paper, we show the design and simulation testing of a control algorithm to mitigate blade, tower, and drivetrain loads using advanced state-space control design methods. The controller uses independent blade pitch to regulate the turbine's speed in region 3. It is also designed to mitigate asymmetric wind disturbances across the rotor disk and add active damping to the tower's first fore-aft mode. In addition, a separate generator torque control loop is designed to add active damping to the tower's first side-side mode and the first drivetrain-torsion mode. This paper describes the test we conducted on the region 3 controller through simulation and outlines steps for future implementation and field tests in the Controls Advanced Research Turbine at the National Renewable Energy Laboratory.

---

† Senior Engineer, National Wind Technology Center, 1617 Cole Blvd., Mailstop 3811, AIAA member

‡ Senior Lecturer, AIAA member

I. Introduction

Typical variable-speed wind turbines have different regions of operation. In below-rated wind speeds (Region 2), blade pitch is held constant, and generator torque control is used to vary the speed of the turbine to maximize energy capture. In above-rated wind speeds (Region 3), generator torque is held constant, and blade-pitch control is used to limit aerodynamic power to maintain constant turbine speed. Another important goal of turbine control is to reduce structural dynamic loads in both operating regions.

Using control to add active damping to flexible turbine modes can reduce fatigue loads. The tower bending modes in particular benefit from active damping. We are interested in the potential benefits of using the generator torque and blade pitch actuators to actively damp the tower's side-side (s-s) and fore-aft (f-a) bending modes. These controllers will require an additional measurement, such as tower-top acceleration. In Region 3, classical control design methods have been used to design controllers to add damping to the tower's first f-a mode with blade pitch.[1,2] These methods use a notch filter to provide a pitch component which adds active damping to that mode. Similar methods could also be used to actively damp the tower's first s-s mode with generator torque control, although these methods are not discussed in the literature.

In previous papers, we have shown the design of state-space controllers to regulate turbine speed in Region 3 and enhance damping of flexible turbine modes.[3–6] Those papers showed the advantages of using full-state feedback to place turbine plant poles to enhance transient response and increase stability. When turbine measurements are limited, we estimated states. Without state estimation, every state contained in the linear control design model must be measured, which is not practical for most commercial turbines. Successful use of state estimation is based on a few turbine measurements such as generator speed and tower-top acceleration.

Another way to mitigate turbine loads is through independent pitch control, where each blade is pitched independently. Both classical control design and multivariable control design approaches have been used to design independent pitch controls to mitigate the effects of asymmetric wind distributions across the rotor disk.[7,8] In the classical design approach, two separate single-input, single-output (SISO) control loops were used to mitigate the "tilt" and "yaw" oriented loads in the fixed frame using independent pitch.[7] This work was extended with alternative sensors to measure the asymmetrical loading on the rotor.[8] Good results were obtained provided suitable sensors were used. In other work, state-space methods were used to design controls to mitigate vortex/wind turbine interaction.[9] That study included a wind disturbance model that incorporated very detailed vortex characteristics in a full state feedback control law. Fatigue equivalent loads were reduced by as much as 30% compared to a standard proportional-integral (PI) controller. In other work, state-space methods were used to design controls that maximize energy extraction and reduce fatigue loads in Region 2 using pitch control.[10] In that study, independent pitch control was shown through simulation to reduce blade fatigue damage equivalent loads (DELs) by 11%.

Actual field implementation on pitch controlled turbines has verified the capability of state estimating controls to mitigate loads.[11-13] In addition, actual tests have shown that generator torque is an effective control actuator that actively damps the first drivetrain torsion mode in Region 2.[14] Through implementation and field tests we have shown that generator torque and blade pitch can be used together in a single multiple-input, multiple-output (MIMO) control loop to add active damping to the tower's first s-s mode as well as the first f-a mode in region 2.[17]

Other field implementations of controls on the Controls Advanced Research Turbine (CART) have sought to improve energy capture in region 2.[15] Adaptive control techniques have been developed to improve Region 2 energy capture compared to the simpler Region 2 torque controls.[16]

In this paper, we show the design and simulation tests of state-space controls to perform multiple control objectives in region 3. The controls are designed to mitigate shear across the rotor disk and add active damping to the tower's first f-a and first s-s bending modes, as well as the first drivetrain torsion mode. An independent pitch controller performs the function of asymmetric load mitigation (due to windshear) and active damping of the tower's f-a mode. A separate generator torque control loop performs active damping of the first tower s-s mode and the first drivetrain torsion mode. The controllers use perturbations in generator torque and blade pitch to apply this active damping. Typical measurements needed for this control are generator speed, blade root bending moments (of each blade), and tower-top f-a and s-s acceleration. We restrict attention in this paper to design of control for Region 3. The controller is based on full state feedback but uses state estimation based on these measurements.

We also describe steps taken in the control design process, show simulation tests of the controller, and discuss planned steps to implement this controller on the CART at the National Wind Technology Center (NWTC).

II. CART Configuration

The CART (Fig. 1) is a two-bladed, teetered, upwind, active-yaw wind turbine. This machine is used as a test bed to study aspects of wind turbine control technology for medium- to large-scale machines.[15]

The CART is variable speed, and each blade is capable of being independently pitched with its own electromechanical servo. The pitch system can pitch the blades up to 18 degrees per second (deg/s) with pitch accelerations up to 150 degrees per second. The squirrel cage induction generator with full power electronics can control torque from minus rating (motoring) to plus rating (generating) at any speed. The torque control loop has a very high-rated bandwidth of 500 radians per second (rad/s).

Figure 1. The controls advanced research turbine (CART).

Rated electrical power (600 kilowatts at a low-speed shaft [LSS] speed of 41.7 revolutions per minute [rpm]) is maintained in Region 3 in a conventional variable-speed approach. Power electronics are used to command constant torque from the generator and blade pitch controls the rotor speed.

The machine is equipped with a full complement of instruments that gather meteorological data at four heights. Blade-root flap and edge-strain gages, tower-bending gages, and LSS and high-speed shaft (HSS) torque transducers gather load data. Accelerometers in the nacelle measure the tower's f-a and s-s motion. Absolute position encoders gather data on pitch, yaw, teeter, LSS, and HSS positions. These data are sampled at 100 Hz. The custom-built control system collects these data and controls the turbine at a control loop cycle rate of 100 Hz. This system is personal computer based and very flexible.

One challenge of wind turbine control design is meeting multiple control objectives. While maintaining constant turbine speed in Region 3, we must also reduce dynamic loads to obtain longer turbine lifetimes and reduce the cost of energy. If controls are not carefully designed to account for the flexible modes of the wind turbine, we can actually increase dynamic loads by destabilizing low-damped modes. We now describe the design of state-space controls for Region 3 that allow us to meet the primary objectives in this region, mitigate the effects of asymmetric wind disturbances across the rotor disk, and enhance the damping in the tower's first f-a and s-s modes, as well as the first drivetrain torsion mode.

III. State-Space Control Design

We restrict our attention in this paper to control design in Region 3. The main goal in Region 3 is to control rotor-speed to a desired set-point (rated speed). A second objective for our control is to mitigate the effects of asymmetric wind variations across the rotor disk and to add active damping to the tower's first f-a mode and s-s mode as well as the first drivetrain torsion mode.

The independent blade pitch control will regulate turbine speed, mitigate asymmetric wind disturbances across the rotor disk, and actively damp the tower's first f-a mode. A separate generator torque control loop will apply active damping to the tower's first s-s mode as well as the drivetrain's first torsion mode. The independent pitch control and generator torque control will be done in separate control loops (Fig. 2). We first describe the design of the independent blade pitch control loop.

A. Independent Blade Pitch Control Design

The objectives of the Region 3 independent blade pitch control algorithm are to regulate speed to 41.7 revolutions per minute (rpm) and to add active damping to the tower's first f-a bending mode. An additional goal is to mitigate the effects of asymmetric wind disturbances across the rotor disk. This independent blade pitch controller will perform the above control objectives in a single loop (but separate from the generator torque control loop to be described below). As described above, the CART is a two-bladed teetering hub machine. We will assume that the teeter degree of freedom (DOF) is locked in the design of this independent blade pitch controller.

All of our control designs will be based on linear time invariant (LTI) state-space control design methods. This means that we design our controls from a linear model of the turbine generated at a particular Region 3 turbine operating point.

A linear time-invariant state-space model describing the CART dynamics and used for control design can be described as:

$$\begin{aligned} \dot{\underline{x}} &= A\underline{x} + B\underline{u} + B_d\underline{u}_d \\ \underline{y} &= C\underline{x} + D\underline{u} + D_d\underline{u}_d \end{aligned} \tag{1}$$

where $\underline{u}$ is the vector of control inputs: perturbed pitch rate of each blade to be described shortly. The vector $\underline{u}_d$ is the disturbance input. $\underline{x}$ and $\underline{y}$ are the state vector and measurement vector respectively, described below. The matrix A is the state matrix, B is the control input transmission matrix, B_d is the disturbance input transmission matrix, C relates the measurements to the states, D relates the measurements to the control input, and D_d relates the measurements to the disturbance inputs. The state matrices A, B, B_d, C, D, and D_d are found by linearizing a FAST aeroelastic model about an operating point in Region 3.[18]

We base our independent pitch control design on Disturbance Accommodating Control (DAC).[19] The basic idea of DAC is the augmentation of the usual state-estimator-based controller to recreate disturbance states via an "assumed-waveform" model. These disturbance states are used as part of the feedback control to reduce ("accommodate") or counteract any persistent disturbance effects.[19]

We assume a disturbance generator in the form of an additional state-space model for the disturbance alone, described by:

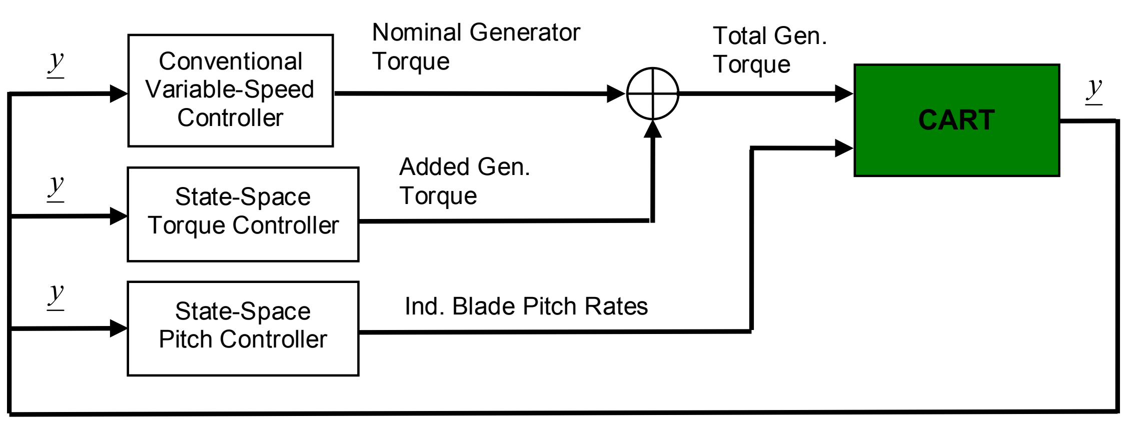

Figure 2. State-space controller architecture.

$$\begin{aligned}\dot{\underline{z}}_d(t) &= F\underline{z}_d(t)\\ \underline{u}_d(t) &= \Theta\underline{z}_d(t)\end{aligned}. \tag{2}$$

where $\underline{z}_d$ is the disturbance state vector, F is the disturbance generator state matrix, and Θ relates the disturbance $\underline{u}_d(t)$ to the disturbance states.

We include two wind disturbances in the vector $\underline{u}_d$ in Eq. (1), a disturbance representing the linear part of the wind shear, and a disturbance uniform over the rotor disk.[20] The linear shear disturbance terms will provide independent blade pitch commands that will mitigate the effects of shear variations across the rotor disk. For example, when the turbine is operating in the presence of a vertical shear profile, the wind speed at the top of the rotor is different than at the bottom. To mitigate this effect, the blade pitch angle must be different when the blade is straight up than when it is straight down. This can only be accomplished if the pitch of each blade is controlled "independently." The uniform disturbance will induce rotor collective pitch commands, which improve speed regulation.

$$\underline{u}_d = \begin{bmatrix} u_{d_1}(t) \\ u_{d_2}(t) \end{bmatrix} = \begin{bmatrix} \text{linear shear disturbance} \\ \text{uniform wind disturbance} \end{bmatrix}. \tag{3}$$

A state-space model for the disturbance can be described by Eq. (2), with

$$\theta = \begin{bmatrix} 1 & 0 & 0 \\ 0 & 0 & 1 \end{bmatrix},\ F = \begin{bmatrix} 0 & 1 & 0 \\ -\Omega^2 & 0 & 0 \\ 0 & 0 & 0 \end{bmatrix},\text{ and } \underline{z}_d = \begin{bmatrix} \text{z}_{\text{d}_1}\text{ -linear shear disturbance state1} \\ \text{z}_{\text{d}_2}\text{ -linear shear disturbance state2} \\ \text{z}_{\text{d}_3}\text{ -uniform wind disturbance state} \end{bmatrix}.^{20} \tag{4}$$

Here, Ω is the nominal rotor-speed set-point (41.7 rpm). Two disturbance states are needed to describe the linear shear variation across the rotor disk, while just one disturbance is needed to describe the uniform wind disturbance across the rotor disk.[20]

The vector of plant states $\underline{x}$ for this control model can be described by

$$\underline{x} = \begin{bmatrix} \text{perturbed tower 1}^{\text{st}}\text{f-a bending deflection} \\ \text{perturbed blade 1 flapwise deflection} \\ \text{perturbed blade 2 flapwise deflection} \\ \text{perturbed tower 1}^{\text{st}}\text{f-a bending velocity} \\ \text{perturbed generator speed} \\ \text{perturbed blade 1 flapwise velocity} \\ \text{perturbed blade 2 flapwise velocity} \\ \text{blade 1 perturbed pitch angle} \\ \text{blade 1 perturbed pitch rate} \\ \text{blade 2 perturbed pitch angle} \\ \text{blade 2 perturbed pitch rate} \end{bmatrix} \tag{5}$$

We include states in Eq. (5) representing the blade-1 and blade-2 perturbed pitch angle and rate to model actuator dynamics, which is important for implementation of pitch control into the CART.[12] In that paper, we described the CART actuator model for our control models. In this context, "perturbed" refers to small deviations of the states, control inputs, disturbance inputs, and measurements from the turbine linearization point.

The control input $\underline{u}$ consists of the perturbed pitch rate of each blade:

$$\underline{u} = \begin{bmatrix} \text{perturbed blade 1 pitch rate} \\ \text{perturbed blade 2 pitch rate} \end{bmatrix} \tag{6}$$

We select the following five CART measurements:

$$\underline{y} = \begin{bmatrix} \text{perturbed generator speed} \\ \text{perturbed blade-1 pitch angle} \\ \text{perturbed blade-2 pitch angle} \\ \text{perturbed tower-top fore-aft acceleration} \\ \frac{1}{2}\text{(blade-1 root flapwise bending moment - blade-2 root flapwise bending moment)} \end{bmatrix} \tag{7}$$

The last measurement in $\underline{y}$ requires further explanation. We need some measurement that captures the effects of the first asymmetric flap mode to ensure observability of this state-space system.[20] We could choose measurement of the first asymmetric flap mode tip-deflection (the first asymmetric flap mode can be obtained by a transformation of the first flap mode of each individual blade; we would thus measure the tip deflection of each blade).[20] Another possible measurement is the difference in the blade-1 and blade-2 root flap-wise bending moment. Because the blade-tip flap deflections are almost impossible to measure on current machines, we measure the blade-root flap-bending moments instead of tip deflections in this study. Future studies will investigate alternative sensors for this state-space control.

Based on the state-space CART model, a state estimator is formed:

$$\dot{\hat{\underline{x}}} = \left(A - KC\right)\hat{\underline{x}} + B\underline{u} + B_d\hat{\underline{u}}_d + K\underline{y} \tag{8}$$

where $\hat{\underline{x}}$ is the estimate of plant states, $\underline{u}$ is the control input described by Eq. (6), $\underline{y}$ are the measurements described by Eq. (7), and $\hat{\underline{u}}_d$ is the disturbance estimate. Full-state feedback is used to produce controller commands for independent blade pitch rate. The matrix K is the matrix of state estimator gains.

We base our control design on the feedback law:

$$\underline{u}(t) = G\ \hat{\underline{x}}(t) + G_d\ \hat{\underline{z}}_d(t) \tag{9}$$

This feedback law is based on estimates ($\hat{\underline{x}}$, $\hat{\underline{z}}_d$) of the plant and disturbance states instead of the actual states themselves ($\underline{x}$, $\underline{z}_d$). State estimation allows us to perform full state feedback by measuring a subset of the states or linear combinations of the states, disturbances and control inputs. This allows us to greatly reduce the number of turbine measurements needed to perform this control.

To calculate the gain matrix G and the state estimator gain matrix K, we use the linear quadratic regulation (LQR) method in MATLAB.[21] This approach for gain calculation allows us to trade off state regulation with actuator effort. To add tower f-a damping in particular, the states that correspond to tower-top f-a rates of deflection are weighted most heavily. We do not include the wind disturbance states in this LQR calculation, since these states are involved with the calculation of G_d (see Eq. [9]), which is calculated independently of G.

The gain G_d is chosen to minimize the effects of disturbances. Note that in this control model, G_d will have three components $\left[G_{d_1}\ G_{d_2}\ G_{d_3} \right]$, corresponding to the three disturbance states described in Eq. (4) for $\underline{z}_d$. The first two gains correspond to the states representing the linear shear disturbance, and the last gain corresponds to the uniform wind disturbance state.

The controller was designed from a linear state-space model described above for the Region 3 operating point defined by a rotor speed of 41.7 rpm, hub-height wind speed of 18.0 meters per second (m/s), and a pitch angle of 11 degrees (deg.). Table 1 compares the open-loop values of the poles to the closed-loop values of these poles after full state feedback. The highlighted poles (red) illustrate how we increased damping through full state feedback to improve stability and transient response.

Table 1. Open-loop and Closed-loop Pole Locations with Independent Blade Pitch Control

	Open-loop poles	Closed-loop poles
First flap symmetric mode	−3.63 ± 13.81i (rad/s)	−3.66 ± 13.85i (rad/s)
First flap asymmetric mode	-3.65 ± 13.32i	−3.65 ± 13.32i (rad/s)
Tower first f-a mode	−0.07 ± 5.52i (rad/s)	−0.65 ± 5.46i (rad/s)
Generator speed	−0.1943	−1.69
Blade-1 actuator pitch	0	-10.0
Blade-2 actuator pitch	0	-10.1
Blade-1 actuator pitch rate	-60	-59.5
Blade-1 actuator pitch rate	-60	-59.5

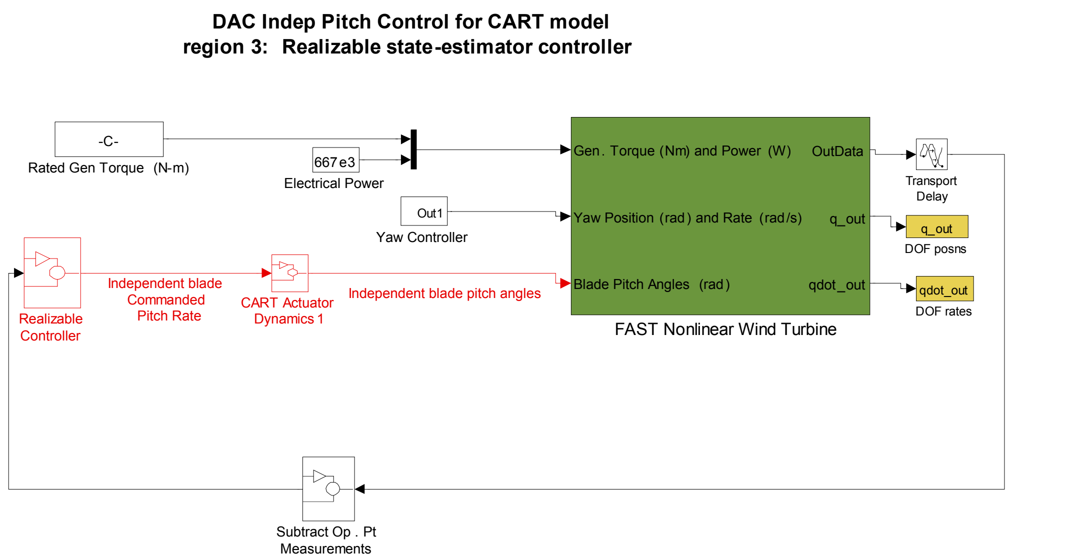

Figure 3. Simulink-FAST model of the closed-loop system with realizable independent pitch controller.

We performed simulations of the resulting controller in closed-loop with a FAST model of the turbine imbedded in a Simulink model.[18] Figure 3 shows a Simulink model of the closed-loop system for simulation. Please note that since we have assumed that the teeter DOF is absent (locked teeter), we switched this DOF off in all of the simulations shown in this paper.

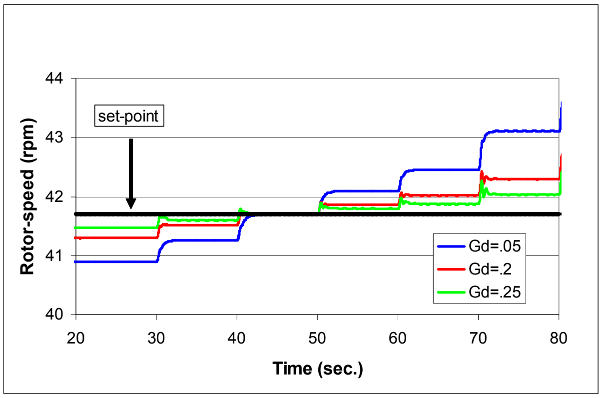

Figure 4. Simulated rotor-speed in response to a step wind input for various values of G_d.

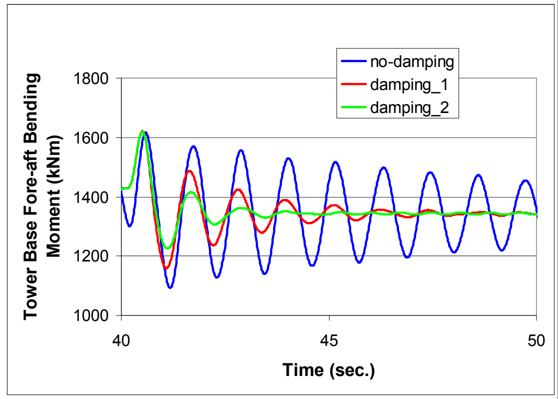

Figure 5. Simulated tower bending moment in response to step wind input for various values of gain.

We excited the model with step changes in wind speed, representing the uniform wind disturbance (without shear) across the rotor disk. Figure 4 shows speed regulation for various values of the gain G_{d_3} associated with the state corresponding to the uniform wind disturbance. The wind speed starts at 16 meters per second (m/s) in the 20 – 30 s interval and increases in steps up to 24 m/s in the 70 – 80 s interval. The wind speed equals 18 m/s (the control design point wind speed) in the 40 – 50 s interval. The controller regulates rotor speed exactly to the set point (41.7 rpm) only in this interval. For other intervals, the regulated rotor speed differs from the set point. We see improved speed regulation performance for increasing values of G_{d_3}.

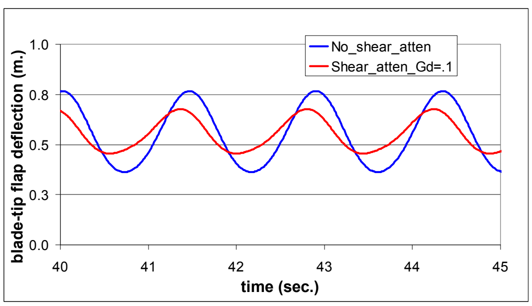

Figure 6. Simulated blade-tip flap deflection excited by linear vertical wind shear.

Next, we examine the effects of active tower damping with pitch control. Figure 5 shows the tower's f-a bending moment at the tower base. At t=40 s, a step change in wind speed occurs that excites the tower f-a motion. The response is oscillatory at the tower's first f-a natural frequency and decays depending upon the amount of damping in the system. The blue plot represents the case of open-loop damping; no damping is added by the controller. For this case, the poles are located as shown in Table 1 with real parts at −0.07. The other two cases represent active tower damping from control, with the real parts of the tower's first f-a mode located at −0.47 in the "damping_1" case and −0.65 for the "damping_2" case. Adding active damping causes the transient response to decay faster than for the open-loop damping case. This active damping should provide a tower load mitigating capability as we will see in another section.

Next, we tested the capability of this controller to mitigate the effects of a wind-shear distribution across the rotor disk. For this simulation test, we applied constant wind speed at 18 m/s but with a vertical wind shear described by a power-law coefficient equal to 0.4 during the entire simulation. Figure 6 shows the blade-tip flap deflection. We simulated various values of the gains G_{d_1} and G_{d_2} associated with the shear disturbance states and chose the values which gave the most attenuation of the cyclic content of the blade-tip flap deflection due to wind shear. The "No_shear_atten" case is for $G_{d_1} = 0$ and $G_{d_2} = 0$. The case "Shear_atten_1" represents $G_{d_1} = 0.1$ and $G_{d_2} = 0$. We note the reduction in cyclic amplitude of the blade-tip flap response for the case with shear disturbance attenuation.

Having tested the independent pitch control loop with simple preliminary simulations, we proceed to design the generator torque control as a separate control loop.

B. Generator Torque Controller

The main goal of Region 3 torque control is to maintain constant generator torque. A second objective for our control is to add active damping to the tower's first s-s mode as well as the drivetrain first torsion mode. We apply the state-space controls as perturbations of torque added on to the conventional Region 3 constant torque. This controller is designed separately from the independent pitch controller; the linear model used for design of this controller is different from the linear model used to design the independent pitch controller.

The state-space model of the CART for design of the generator torque control is described by Eq. (1) without the disturbance $\underline{u}_d$ (for the generator torque controller we do not need to mitigate shear or uniform wind disturbances as with the independent pitch controller). Now $\underline{u}$ consists of the perturbed generator torque as the single control input instead of independent pitch. The state matrices (*A*, *B*, *C,* and *D*) are found by linearizing a FAST aeroelastic model at the same operating point selected for the independent pitch control design.

Seven state variables in $\underline{x}$ are chosen to characterize the structural dynamics of interest for this generator torque linear control design model. These state variables include:

$$\underline{x} = \begin{bmatrix} \text{perturbed tower first s-s bending deflection} \\ \text{perturbed drivetrain first torsional deflection} \\ \text{perturbed tower first s-s bending velocity} \\ \text{perturbed generator speed} \\ \text{perturbed drivetrain first torsional velocity} \\ \text{tower-top acceleration filter state 1} \\ \text{tower-top acceleration filter state 2} \end{bmatrix} \tag{10}$$

The inputs (measurements) to the state estimator controller are:

$$\underline{y} = \begin{bmatrix} \text{perturbed generator speed} \\ \text{perturbed tower-top s-s acceleration} \end{bmatrix} \tag{11}$$

From previous studies, we know that the tower s-s accelerometer data used for the measurement in Eq. (11) contains high frequency noise.[17] If this signal is used as an input to the controller; the commanded generator torque also contains high frequency noise, which is highly undesirable. We must first filter this signal before using it as an input to the controller. Even a filter that attenuates high-frequency noise can change the phase of a signal at low frequencies (such as the tower first s-s frequency). We are concerned with this phase shift because it causes the commanded generator torque to be applied at the wrong phase and destabilizes the tower's s-s motion. This phase effect must be accounted for in the controller so that torque commands will be applied at the correct phase. One way to do this is to represent a model of the filter in the linear model used for control design and to add these filter states to the state vector.[17] In this way, the controller has the information it needs about the filter to apply torque fluctuations at the correct phase angle to stabilize the tower's s-s motion.

We chose the following filter for this control:

$$F(s) = \frac{0.03\, s + 30.0}{s^2 + 15.0\, s + 30.0} \tag{12}$$

This filter provides the characteristics necessary to attenuate accelerometer response at high frequency.

The goal of state-space control design is to use full state feedback to place the poles of the plant to improve stability and transient response. Without full state feedback, the eigenvalues of the matrix at this operating point have the open-loop pole values shown in Table 2. We used LQR to design this controller.[22] The largest weightings were placed on the states that corresponded to the tower's first s-s mode as well as the drivetrain's first torsion mode. As a result, these poles are moved farther to the left in the complex plane for improved damping. We place only small weighting on the state that corresponded to the generator speed state. Table 2 summarizes the open- and closed-loop pole locations. The values in red show how we improved damping through full state feedback.

Our next step is to test this control loop separately from the pitch control loop. We want to be sure that the controller is meeting the objective of active damping of the tower's first s-s mode and the drivetrain's first torsion mode. In this simulation, we apply a constant wind speed equal to the control design point wind speed of 18 m/s. We remove the pitch controller and just apply constant pitch equal to the control design point pitch angle of 11 deg. Because the rotor speed, pitch angle, and wind speed are all equal to the values at the control design point, no pitch control is necessary as the closed-loop system will be operating at this stable equilibrium point. In this way, we can test just the torque control loop.

Table 2. Open-loop and Closed-loop Pole Locations with Generator Torque Control

	Open-loop poles	**Closed-loop poles**
Tower first s-s mode	−0.002 ± 5.54i (rad/s)	−0.198 ± 5.54i (rad/s)
Generator speed	−0.102	−0.102
Drivetrain first torsion	−0.01 ± 22.47i (rad/s)	−1.08 ± 22.45i (rad/s)
Filter state 1	-12.62	-12.62
Filter state 2	-2.38	-2.38

Figure 7 shows the Simulink model used for this simulation with the generator torque state-space controller shown in red. To excite the flexible modes (the tower's first s-s mode and the drivetrain's first torsion mode), we added an impulse at t=50 s. Figure 8 shows the simulated tower s-s bending moment at the tower base. In this figure we show two plots, one for the case without active damping and one for the case with active damping from the controller. The large reduction in tower s-s bending moments with active control is readily seen. Figure 9 shows the simulated low-speed shaft torque loads for the same two cases. For the case with active damping, the response decays about 3 s after application of the impulse at t=50s. For the case without damping, the response keeps "ringing" at the drivetrain's first torsional frequency because of the small amount of open-loop damping. This simulation verified that the generator torque state-space controller satisfies the objectives for which it was designed.

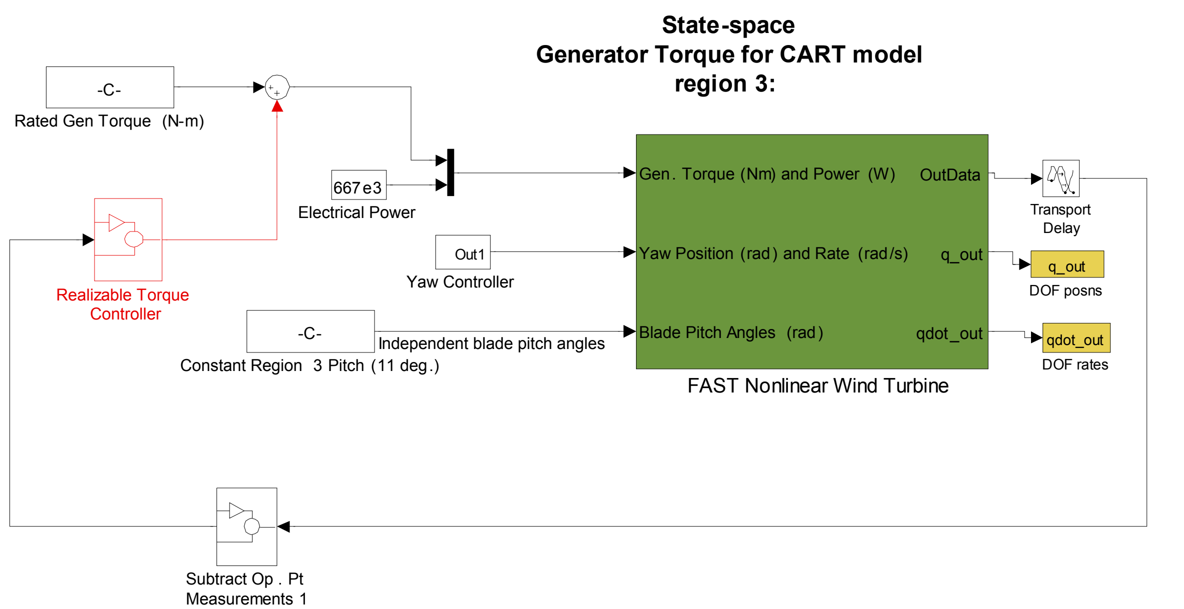

Figure 7. Simulink-FAST model of the closed-loop system with generator torque realizable controller.

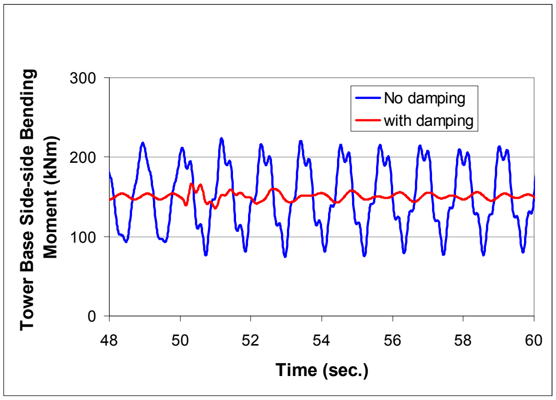

Figure 8. Simulated tower s-s moment with and without damping from generator torque control; no pitch control.

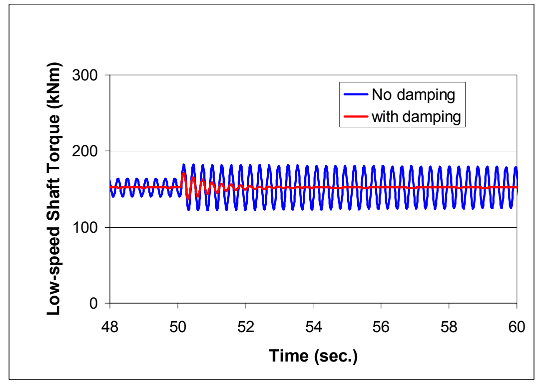

Figure 9. Simulated low-speed shaft torque with and without damping from generator torque control; no pitch control.

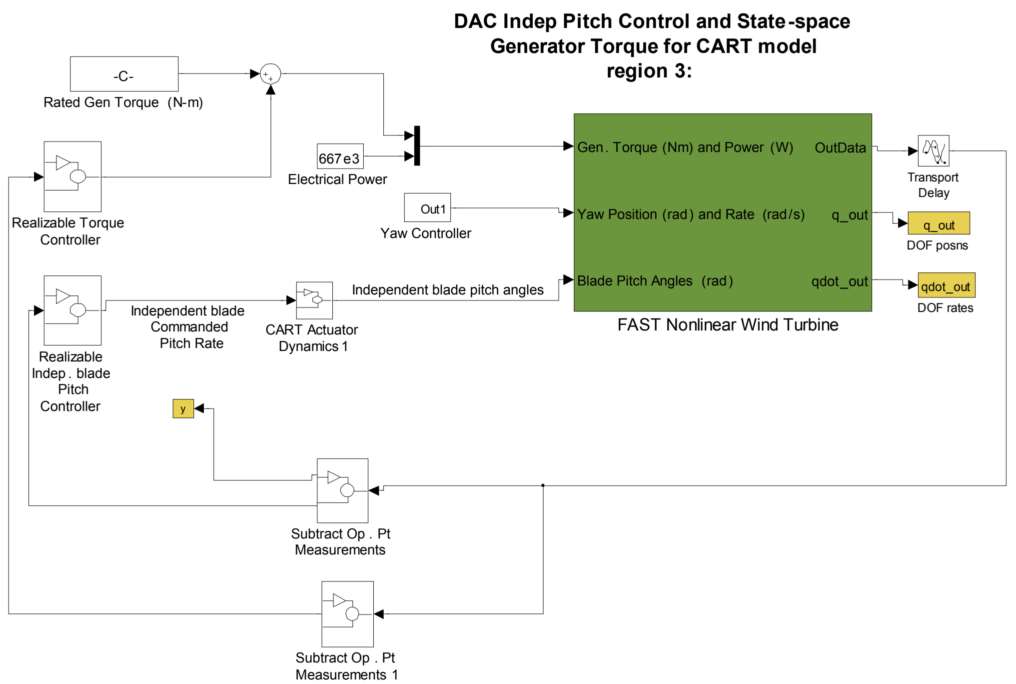

Figure 10. Simulink-FAST model of the closed-loop system with generator torque and blade independent pitch realizable controllers.

Our next test was to put both of these controllers together to be sure that the two loops do not interact in an undesirable way. Figure 10 shows the Simulink model used for simulation with both control loops present. In this simulation, we excite the closed-loop system with step winds with a superimposed constant wind shear (power law exponent of 0.4) (we did not apply impulses as we did in the last simulation). The step winds varied in the same way as the simulations shown previously for the blade independent pitch controller test. In the following plots we will show two cases: the "without damping or shear mitigation case" and the "with damping and shear mitigation case." In the "without damping or shear mitigation" case, the state-space generator torque controller was disconnected in the Simulink model. The pitch controller was redesigned with zero weighting on the tower's first f-a velocity states and the two shear disturbance gains set to zero. This effectively left only a component of collective pitch control to mitigate the effects of the uniform disturbance and provide overall speed regulation with constant generator torque. The "with damping and shear mitigation" case represents full control with both the generator torque control loop and the independent blade pitch control loop active and with shear mitigation and active tower damping occurring as originally designed.

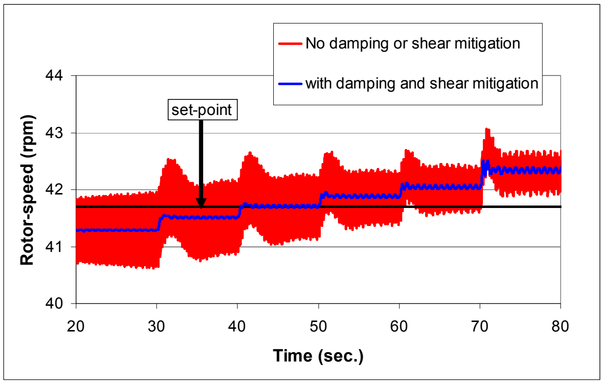

Figure 11. Simulated rotor speed with and without active damping and shear mitigation from pitch control.

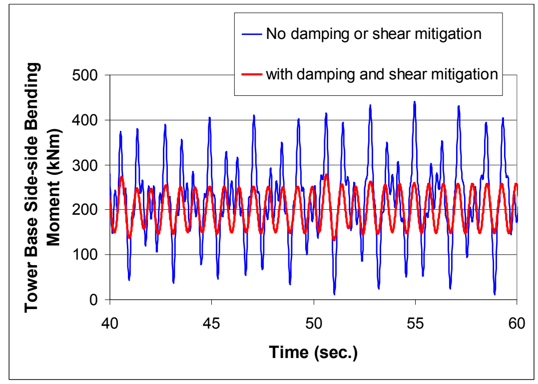

Figure 12. Simulated tower s-s moment with and without damping from generator torque control and shear mitigation from pitch control; generator torque and pitch together.

Figure 11 shows speed regulation for these two cases. In the "no damping or shear mitigation case," there are significant cyclic variations in rotor-speed because of the effects of the wind shear, first drivetrain torsion vibrations and tower vibrations. In the case "with damping and shear mitigation," these high frequency variations are greatly reduced because of the active damping and shear mitigation.

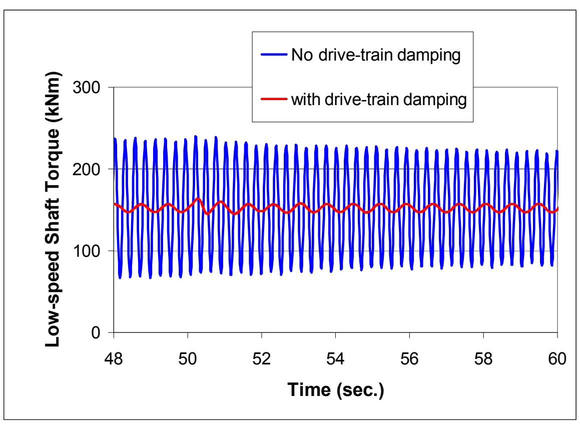

Figure 13. Simulated low-speed shaft torque with and without damping from generator torque control; generator torque and pitch together.

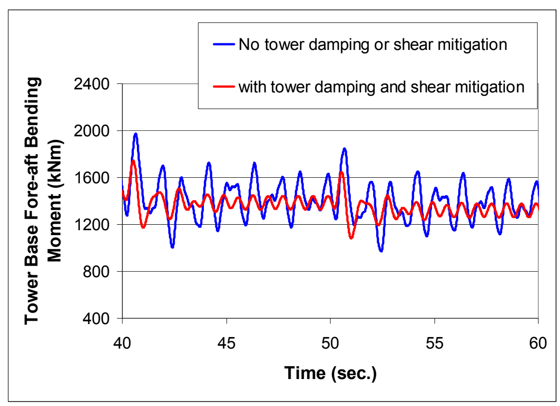

Figure 14. Simulated tower f-a bending moment with and without active damping and shear mitigation from pitch control.

Figure 12 shows the simulated tower base s-s bending moments for these two cases. The mitigation of these loads for the case with damping and shear mitigation is readily evident. This shows that the generator torque controller is successfully applying active damping to the tower's first s-s bending mode. In addition, some of this load mitigation comes from the independent pitch control shear mitigation because the asymmetric rotor loads produced by the wind shear are transferred to the tower's s-s bending moment.

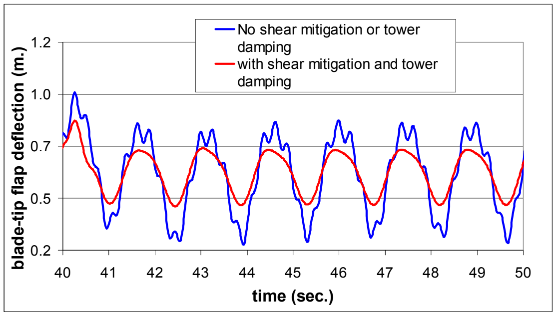

Figure 15. Simulated blade-tip flap deflection with and without shear mitigation from pitch control.

Figure 13 shows the simulated low-speed shaft torque loads. The loads for the case with drivetrain damping are significantly less than the loads without drivetrain damping. Figure 14 shows the simulated tower base f-a bending moments with significant load reduction for the case when tower damping and shear mitigation are applied. Figure 15 shows the simulated blade-tip flap deflections with a reduction in deflections for the case when shear mitigation is applied.

From this simulation, it appears that the two control loops do not interact in an undesirable way, and that the control objectives are met. These simulations with simple step winds and wind shear are preliminary. To fully test the control objectives through simulation, we need to apply turbulent wind inputs to simulate the system in a more realistic environment. Next, we describe simulation tests with turbulent wind inflow.

IV. Turbulent Wind Simulation Tests

We proceed to test the controller in simulations with the effects of turbulent wind inflow. We want to see if the DAC independent pitch and generator torque control loops remain stable in the presence of turbulent wind inflow. We also ascertain if this control scheme mitigates fatigue loads for a turbulence case typical of conditions seen at the NWTC.

We generate turbulent winds using the *Turbsim* stochastic inflow turbulence code.[23] Its purpose is to provide the wind turbine designer with the ability to drive design codes such as FAST simulations with simulated inflow turbulence that incorporate many of the important fluid dynamic features known to adversely affect turbine aeroelastic response and loading. *Turbsim* can generate a turbulent inflow that is characteristic of the highly turbulent conditions experienced when testing turbines at the NWTC; i.e., downwind of a major mountain range.

To generate the turbulent inflow case for this simulation, we use the National Wind Technology Center Upwind (NWTCUP) Spectral Model in *Turbsim*.[23] It represents a test environment corresponding to those found in complex terrain situations that often present challenges for turbine operations. The NWTCUP model incorporates additional scaling features to better reflect conditions seen at the NWTC (high turbulence intensities and intense coherent turbulent structures encountered during stable, nighttime flows).[23] Table 3 shows some of the characteristics of the turbulence time series for this simulation.

We proceed to simulate the controller-turbine system excited by this turbulent inflow. We compare two control cases. Case 1 represents both state-space control loops active with full tower f-a, tower s-s and first drivetrain active damping as well as shear mitigation. Case 2 represents use of a simple proportional-integral (PI) collective pitch controller which only regulates speed in region 3. It does not provide any active tower or drive-train damping and does not mitigate the effects of shear. We adjusted the PI control gains to give similar speed regulation performance to the state-space controller.

Table 3. Summary of the *Turbsim* Generated Turbulence

Specification	Value
Analysis time [seconds]	600
Hub height [m]	37.0
Grid height [m]	65.0
Grid width [m]	65.0
Mean wind speed [m/s]	17.0
Power law exponent	0.3
Surface roughness length [m]	0.018
Gradient Richardson number	0.02
Friction or shear velocity [m/s]	0.889
Length of coherent structures [s.]	300
Minimum coherent TKE [(m/s)^2]	30.0

We analyzed the results from these two cases and calculated various performance measures for blade 1, shown in Table 4 for the two cases. The maximum rotor speed gives an indication of speed regulation performance. Both cases 1 and 2 result in the rotor speed exceeding 43 rpm, which would trigger a shutdown in the CART. We could improve speed regulation by redesigning the independent pitch controller with additional LQR weighting on the generator speed state or increased uniform wind disturbance state gain. We also calculate the root mean square (rms) of the rotor-speed error (the rotor speed minus the 41.7 rpm set point), the rms of the pitch rate and the maximum pitch rate, as well as the maximum generator torque.

As can be seen in Table 4, case 1 results in increased blade pitch activity compared to case 2, as reflected in the increase in rms pitch rate and maximum pitch rate. This result is expected because we are adding active damping to the tower's first f-a mode and mitigating the shear across the rotor disk. Figure 16 confirms the increased pitch rates for case 1; with the pitch rates reaching the upper and lower pitch rate limits (± 18 deg/s).

Next we look at demand on the generator torque for this control. As can be seen in the table, the maximum generator torque is higher for case 1 than for case 2. This is due to the generator torque control adding active damping to the tower's first s-s and the drivetrain's first torsion modes. The maximum generator torque for this case is only about 10% higher than for case 2 in which generator torque is constant (3.526 kNm). Figure 17 shows a plot of a portion of the simulation, showing typical cyclic content of the commanded generator torque for the two cases. For case 1, the generator torque consists of the mean torque plus cyclic content corresponding to active damping at the tower's first s-s natural frequency and the drivetrain's first torsional natural frequency.

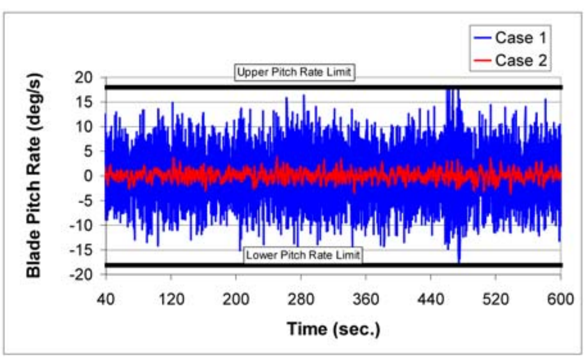

Figure 16. Simulated blade 1 pitch rates for the two control cases.

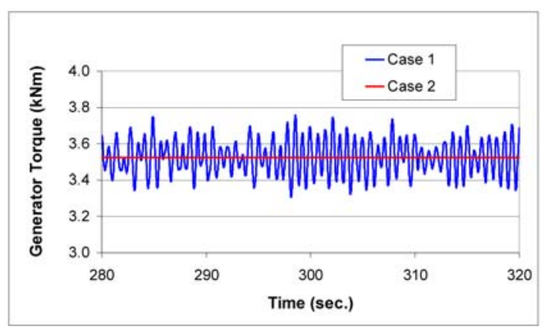

Figure 17. Simulated generator torque for the two control cases.

Next we calculated the fatigue DELs for the tower base f-a and s-s bending moments, the low-speed shaft torque, and the blade root flap-wise-bending moments.[24] Table 4 highlights these results. We note the large reduction in DELs for the tower's s-s bending moments with a more modest decrease for the tower's f-a bending moment and low-speed shaft torque for case 1 compared to case 2. With active damping (case 1), the low-speed shaft torque DEL is reduced by about 28%. The tower's s-s bending moment is reduced by about 79% by this control, and the tower f-a bending moment is reduced by about 21%. The blade-root flap-wise-bending moment is reduced by about 17% with this control, which uses independent pitch to mitigate asymmetric shear disturbances across the rotor disk (case 1). Figure 18 highlights these results. In this plot, we have normalized the results based on case 2 (no active damping or shear mitigation control, which is typical of commercial turbine control) for reference. This figure shows the significant reduction in fatigue DELs for the low-speed shaft and tower. It shows the reduction in fatigue DEL for the blade. These load reductions come at the expense of a modest increase in generator torque activity and a more substantial increase in blade pitch activity.

Table 4: Comparison Between the Two State-Space Control Cases

Performance Measure	Case 1	Case 2
Max rotor-speed (rpm)	43.01	43.02
RMS speed error (rpm)	0.69	0.68
Max pitch rate (deg/s)	18	3.83
RMS pitch rate (deg/s)	4.74	1.02
Max Generator Torque (kNm)	3.88	3.52
Tower f-a fatigue DEL (kNm)	817.47	1029.8
Tower s-s fatigue DEL (kNm)	161.12	779.23
Low-speed shaft torque fatigue DEL (kNm)	24.15	33.51
Blade-root flap-bending moment fatigue DEL (kNm)	210.55	252.61

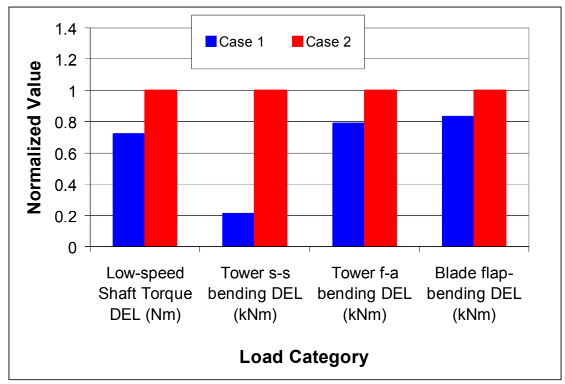

Figure 18. Illustration of case 1 and case 2 results.

V. Conclusions

In this paper, we have shown the design, implementation, and testing of a Region 3 state-space control algorithm for fatigue load mitigation. The Region 3 control objectives are performed with two separate control loops. An independent blade pitch controller regulates turbine speed to a required set-point, mitigates the shear distribution across the rotor disk, and adds active damping to the tower's first f-a mode. A separate generator torque control loop adds active damping to the tower's first s-s and drivetrain's first torsion mode. This active damping and shear mitigation reduce Region 3 fatigue loads.

We showed the linear time invariant control design methods used for the design of these two separate state-space controllers. We also showed simulation tests to verify the performance of these controllers. We started with simple step wind inputs and progressed to more sophisticated simulation tests with turbulent wind inflow.

For the turbulent wind inflow case, we calculated fatigue damage equivalent loads for the low-speed shaft torque, the tower's f-a and s-s base bending moments, and the blade root flap-wise-bending moment. We compared results from this controller to results from a PI controller designed only to regulate turbine speed in region 3. Results from the state-space controller showed a 79% reduction in the tower's s-s bending load, a 21% reduction in the tower's f-a bending load, a 28% reduction in drivetrain torque loads, as well as a 17% reduction in the blade root flap-wise bending moment loads compared to the PI control case. The measurements for this state-space controller include generator speed, tower-top f-a and s-s acceleration, the pitch angle of the two blades, and the root flap-wise-bending moments on the two blades (we actually input the difference between the bending moment on blade 1 and the bending moment on blade 2). We noted that the pitch rates for the controller with active damping and shear mitigation were higher than for the PI control case. For the simulation tests we conducted there were a limited number of occurrences when the pitch rates reached or exceeded the pitch rate limits for the state-space controller. The increased requirements on generator torque for active damping of the tower's s-s mode and the drivetrain's first torsion mode for the state-space controller were modest, well within the capabilities of this generator.

Future Work

Having now designed and tested the above controller through simulation, we will proceed to field implement and test this controller in the CART. We will perform these tests in the CART with the teeter degree of freedom locked. Since we have never tested the turbine in this configuration, we will need to collect baseline data in which there is no active tower damping or shear mitigation for comparison purposes.

We will first implement and test the independent blade pitch controller without the state-space generator torque controller (we will apply constant region 3 generator torque). We will first set the tower f-a damping and shear mitigation gains in the independent pitch controller to zero and test just the speed regulation component. The control actions for this part of the controller should be predominately collective pitch because the only function is speed regulation. The speed regulation performance will depend upon the gain chosen for the uniform wind disturbance as well as the LQR weighting placed on the generator speed state. We will collect several ten minute data-sets to use as a baseline for comparison to the results when active tower f-a damping and shear mitigation are active.

Next we will add active tower f-a damping by redesigning the controller with non-zero weighting on the tower first f-a velocity state. We will collect several data-sets and compare the results from this control to baseline results with no tower f-a damping to assess the degree to which this controller mitigates tower f-a bending fatigue loads.

Next we will "switch on" active shear mitigation by choosing appropriate shear disturbance gains and redesigning the independent pitch controller. We will compare to the data-sets already collected with the shear disturbance gains set to zero to assess the blade load mitigating potential of this controller.

The next step will be to add the generator torque controller. We will collect several data-sets and compare to the data already collected in which the generator torque is constant. We will assess the degree to which this controller mitigates the drivetrain torque and tower s-s bending loads. We will also ascertain whether this controller interacts with the independent blade pitch controller in an undesirable way, as these two control loops are separate. If we observe significant undesirable interaction, we will proceed to design and test a single multiple input multiple output controller, which performs all of these control objectives in a single control loop.

We will also investigate alternative sensors for the measurements needed for the independent blade pitch control. We will investigate possible use of sensors for measuring the wind-speed distribution upwind of the turbine, instead of relying on turbine measurements alone for estimation of the disturbance states. We will then begin design and implementation of similar controls for a 3-bladed version of the CART.

References

[1]Bossanyi, E. A., "Developments in Closed Loop Controller Design for Wind Turbines," *19th ASME Wind Energy Conference*, Reno, NV, 2000, pp. 64-74.

[2]Burton, T., Sharpe, D., Jenkins, N., and Bossanyi, E., 2001, *Wind Energy Handbook*, John Wiley & Sons, LTD, New York, pp. 488−489.

[3]Wright, A. D., and Balas, M., "Design of State-Space-Based Control Algorithms for Wind Turbine Speed Regulation," *ASME J. Solar Energy Engineering*, Vol. 125, No. 4, November 2003, pp. 386-395.

[4]Wright, A. D., and Balas, M., "Design of Controls to Attenuate Loads in the Controls Advanced Research Turbine," *ASME J. Solar Energy Engineering*, Vol. 126, No. 4, November 2004, pp. 1083-1091.

[5]Wright, A. D., "Control Design for Flexible Wind Turbines," Ph.D. Dissertation, Department of Aerospace Engineering Sciences, University of Colorado, Boulder, CO, 2003.

[6]Stol, K., and Balas, M., "Periodic Disturbance Accommodating Control for Blade Load Mitigation in Wind Turbines," *ASME J. Solar Energy Engineering*, Vol. 125, No. 4, November 2003, pp. 379-385.

[7]Bossanyi, E. A., "Individual Blade Pitch Control for Load Reduction," Wind Energy, 6: 119-128, 2003.

[8]Bossanyi, E. A., "Developments in Individual Blade Pitch Control," EWEA conference "The Science of Making Torque from Wind," DUWIND, Delft University of Technology, The Netherlands, April 19-21, 2004.

[9]Hand, M. M., and Balas, M. J., "Load Mitigation Control Design for a Wind Turbine Operating in the Path of Vortices," National Renewable Energy Laboratory, NREL/CP-500-35966, Golden, Co. 2004.

[10]Stol, K., "Disturbance Tracking Control and Blade Load Mitigation for Variable-Speed Wind Turbines," *ASME J. Solar Energy Engineering*, Vol. 125, No. 4, November 2003, pp. 396-401.

[11]Stol, K., and Fingersh, L., "Wind Turbine Field Testing of State-Space Control Designs," National Renewable Energy Laboratory, NREL/SR-500-35061, Golden, CO, 2004.

[12]Wright, A., Stol, K., and Fingersh, L., "Progress in Implementing and Testing State-Space Controls for the Controls Advanced Research Turbine," *24th ASME Wind Energy Conference*, Reno, NV, 2005, pp. 88-100.

[13]Stol, K., Zhao, W., and Wright, A., "Individual Blade Pitch Control for the Controls Advanced Research Turbine (CART)," *ASME J. Solar Energy Engineering*, Vol. 128, No. 4, November 2006, pp. 498−505.

[14]Wright, A., Fingersh, L., and Balas, M., "Testing State-Space Controls for the Controls Advanced Research Turbine," *ASME J. Solar Energy Engineering*, Vol. 128, No. 4, November 2006, pp. 506−515.

[15]Fingersh, L., and Johnson, K., "Baseline Results and Future Plans for the NREL Controls Advanced Research Turbine," *23rd ASME Wind Energy Conference*, Reno, NV, 2004, pp. 87-93.

[16]Johnson, K. E., Fingersh, L., Balas, M., and Pao, L. Y., "Methods for Increasing Region 2 Power Capture on a Variable Speed HAWT," *ASME J. Solar Energy Engineering*, Vol. 126, No. 4, November 2004, pp. 1092−1100.

[17]Wright, A. D., Fingersh, L. J., and Stol, K. A., "Design and Testing Controls to Mitigate Tower Dynamic Loads in the Controls Advanced Research Turbine," National Renewable Energy Laboratory, NREL/CP-500-40932, Golden, CO, 2007 (http://www.nrel.gov/docs/fy07osti/40932.pdf).

[18]Jonkman, J. M., and Buhl, M. L., "FAST User's Guide," National Renewable Energy Laboratory, NREL/EL-500-38230, Golden, CO, 2005.

[19]Balas, M.J., Lee, Y.J., and Kendall, L., "Disturbance Tracking Control Theory with Application to Horizontal Axis Wind Turbines," *17th ASME Wind Energy Conference*, Reno, Nevada, 12-15 January, 1998.

[20]Wright, A. D., "Modern Control Design for Flexible Wind Turbines," NREL Report No. TP-500-35816, National Renewable Energy Laboratory, Golden, Colorado, 2004.

[21]Grace, A., Laub, A. J., Little, J. N., and Thompson, C. M., "Control System TOOLBOX for Use with MATLAB," The MATHWORKS, Inc., Natick, Mass., July, 1992.

[22]Kwakernaak, H., and Sivan, R., *Linear Optimal Control Systems*, Wiley Interscience, NY, 1972, pp. 207-237.

[23]Jonkman, B. J., and Buhl, M. L. Jr.., "*Turbsim* User's Guide," NREL Report No. TP-500-41136, National Renewable Energy Laboratory, Golden, Colorado, April, 2007.

[24]Sutherland, H. J., "On the Fatigue Analysis of Wind Turbines," Sandia National Laboratories, SAND99-0089, Albuquerque, NM, 1999

REPORT DOCUMENTATION PAGE

Form Approved
OMB No. 0704-0188

The public reporting burden for this collection of information is estimated to average 1 hour per response, including the time for reviewing instructions, searching existing data sources, gathering and maintaining the data needed, and completing and reviewing the collection of information. Send comments regarding this burden estimate or any other aspect of this collection of information, including suggestions for reducing the burden, to Department of Defense, Executive Services and Communications Directorate (0704-0188). Respondents should be aware that notwithstanding any other provision of law, no person shall be subject to any penalty for failing to comply with a collection of information if it does not display a currently valid OMB control number.

PLEASE DO NOT RETURN YOUR FORM TO THE ABOVE ORGANIZATION.

1. REPORT DATE *(DD-MM-YYYY)*	2. REPORT TYPE	3. DATES COVERED *(From - To)*
January 2008	Conference paper	January 7-10, 2008

4. TITLE AND SUBTITLE
Designing and Testing Contols to Mitigate Dynamic Loads in the Controls Advanced Research Turbine: Preprint

5a. CONTRACT NUMBER
DE-AC36-99-GO10337

5b. GRANT NUMBER

5c. PROGRAM ELEMENT NUMBER

6. AUTHOR(S)
A.D. Wright and K.A. Stol

5d. PROJECT NUMBER
NREL/CP-500-42490

5e. TASK NUMBER
WER8.2006

5f. WORK UNIT NUMBER

7. PERFORMING ORGANIZATION NAME(S) AND ADDRESS(ES)
National Renewable Energy Laboratory
1617 Cole Blvd.
Golden, CO 80401-3393

8. PERFORMING ORGANIZATION REPORT NUMBER
NREL/CP-500-42490

9. SPONSORING/MONITORING AGENCY NAME(S) AND ADDRESS(ES)

10. SPONSOR/MONITOR'S ACRONYM(S)
NREL

11. SPONSORING/MONITORING AGENCY REPORT NUMBER

12. DISTRIBUTION AVAILABILITY STATEMENT
National Technical Information Service
U.S. Department of Commerce
5285 Port Royal Road
Springfield, VA 22161

13. SUPPLEMENTARY NOTES

14. ABSTRACT *(Maximum 200 Words)*
The National Renewable Energy Laboratory is designing, implementing, and testing advanced controls to maximize energy extraction and reduce structural dynamic loads of wind turbines. These control designs are based on a linear model of the turbine that is generated by specialized modeling software. In this paper, we show the design and simulation testing of a control algorithm to mitigate blade, tower, and drivetrain loads using advanced state-space control design methods.

15. SUBJECT TERMS
wind energy; wind turbine; design; system controls

16. SECURITY CLASSIFICATION OF: a. REPORT	b. ABSTRACT	c. THIS PAGE	17. LIMITATION OF ABSTRACT	18. NUMBER OF PAGES	19a. NAME OF RESPONSIBLE PERSON
Unclassified	Unclassified	Unclassified	UL		19b. TELEPHONE NUMBER (*Include area code*)

Standard Form 298 (Rev. 8/98)
Prescribed by ANSI Std. Z39.18

F1147-E(09/2007)